MOLECULAR AND CELLULAR BIOLOGY, June 2007, p. 4293–4305 Vol. 27, No. 12
0270-7306/07/$08.00+0 doi:10.1128/MCB.00031-07

Bcl-X_L/Bax Proteins Direct the Fate of Embryonic Cortical Precursor Cells▽†

Mi-Yoon Chang,[1,2]‡ Woong Sun,[4] Wataru Ochiai,[5] Kinichi Nakashima,[6] Soo-Young Kim,[4] Chang-Hwan Park,[2,7] Jin Sun Kang,[2,7] Jae-Won Shim,[1,2,3] A-Young Jo,[1,2,3] Chun-Sik Kang,[1] Yong-Sung Lee,[1,2,3] Jae-Sang Kim,[8] and Sang-Hun Lee[1,2,3]*

Department of Biochemistry & Molecular Biology, College of Medicine, Hanyang University, Seoul 133-791, South Korea[1]; Institute of Mental Health, College of Medicine, Hanyang University, Seoul 133-791, South Korea[2]; Cell Therapy Research Center, College of Medicine, Hanyang University, Seoul 133-791, South Korea[3]; Department of Anatomy, Korea University College of Medicine, Seoul 136-705, South Korea[4]; Department of Anatomy and Cell Biology, Graduate School of Medicine, Nagoya University, 65 Tsurumai-cho, showa-ku, Nagoya 466-8550, Japan[5]; Laboratory of Molecular Neuroscience, Graduate School of Biological Sciences, Nara Institute of Science and Technology, 8916-5 Takayama, Ikoma 630-0101, Japan[6]; Department of Microbiology, College of Medicine, Hanyang University, Seoul 133-791, South Korea[7]; and Division of Molecular Life Sciences, Ewha Womans University, Seoul 120-750, South Korea[8]

Received 6 January 2007/Returned for modification 5 February 2007/Accepted 28 March 2007

In the developing mouse brain, the highest Bcl-X_L expression is seen at the peak of neurogenesis, whereas the peak of Bax expression coincides with the astrogenic period. While such observations suggest an active role of the Bcl-2 family proteins in the generation of neurons and astrocytes, no definitive demonstration has been provided to date. Using combinations of gain- and loss-of-function assays in vivo and in vitro, we provide evidence for instructive roles of these proteins in neuronal and astrocytic fate specification. Specifically, in Bax knockout mice, astrocyte formation was decreased in the developing cortices. Overexpression of Bcl-X_L and Bax in embryonic cortical precursors induced neural and astrocytic differentiation, respectively, while inhibitory RNAs led to the opposite results. Importantly, inhibition of caspase activity, dimerization, or mitochondrial localization of Bcl-X_L/Bax proteins indicated that the differentiation effects of Bcl-X_L/Bax are separable from their roles in cell survival and apoptosis. Lastly, we describe activation of intracellular signaling pathways and expression of basic helix-loop-helix transcriptional factors specific for the Bcl-2 protein-mediated differentiation.

Bcl-2 family proteins play critical roles in the intracellular signal transduction of apoptosis or programmed cell death (39). They can be divided into two groups as follows, depending on their roles in the regulation of apoptosis: the repressors (e.g., Bcl-2 and Bcl-X_L) and promoters (e.g., Bax, Bcl-X_S, Bak, and Bad) of apoptosis. One of their critical roles is adjusting the number of postmitotic neurons (21) and neural precursors (16) during the development of the nervous system.

Previous studies have also reported that Bcl-2 and Bcl-X_L play a key role in the regenerative process of severed retinal axon by promoting axonal growth and that this effect is not an indirect consequence of its well-known antiapoptotic activity (7, 15). Similarly, overexpression of these antiapoptotic proteins in vitro leads to the acquisition of morphological and functional maturity of postmitotic neurons through enhancement of neurite outgrowths (11, 27) as well as synaptic activity in neurons (12). These findings suggest that the Bcl-2 proteins may have diverse functions in the nervous system in addition to their regulatory role in apoptosis.

In the rodent cerebral cortex, neurogenesis commences at around embryonic day 12 (E12) and peaks around E15 (for a review, see reference 23). Interestingly, the expression of the antiapoptotic proteins Bcl-X_L and Bcl-2, which begins at the time of neural tube formation, increases through the early developmental phase of the brain and peaks during the period of neurogenesis (1, 14). Afterwards, Bcl-X_L continues to be expressed in postmitotic neurons, whereas Bcl-2 expression is not detected in the adult brain. In contrast, the period of Bax expression in the developing brain is coincident with that of astrocyte formation (for a review, see reference 23). In the cerebral cortex, Bax begins to be expressed at E15 to E17 (14), reaching the highest expression level at the peak of astrocyte formation, occurring at postnatal days 0 to 2 (P0 to P2), and the expression declines during postnatal development (14, 35). In addition to the pattern of Bcl-X_L/Bax expression in the developing brain, which appears to be consistent with a role in the differentiation of neurons and astrocytes, we recently observed that overexpression of Bcl-X_L facilitates the in vitro differentiation of mouse embryonic stem cells into the neuronal lineage (27). Furthermore, a Bcl-X_L-mediated increase in neuronal number has been demonstrated for the cultures of neural precursors (17). These findings support the possibility that the determination of neuronal versus

* Corresponding author. Mailing address: Department of Biochemistry & Molecular Biology, College of Medicine, Hanyang University, 17 Haengdang-dong, Sungdong-gu, Seoul 133-791, South Korea. Phone: 82-2-2220-0625. Fax: 82-2-2294-6270. E-mail: leesh@hanyang.ac.kr.

† Supplemental material for this article may be found at http://mcb.asm.org/.

‡ Present address: Molecular Neurobiology Laboratory, McLean Hospital and Harvard Medical School, Belmont, MA 02478.

▽ Published ahead of print on 16 April 2007.

astroglial lineages may be actively regulated by balanced levels of anti- and proapoptotic Bcl-2 family proteins in neural precursor cells.

In this study, we addressed the role of Bcl-X_L and Bax in neural precursor differentiation using in vivo analyses of Bax deletion mice and in vitro cultures of neural precursor cells. The data obtained strongly indicate that Bcl-X_L instructively directs the fate of embryonic cortical precursors towards neurons, whereas Bax instructs the same precursors to undergo astrocytic differentiation.

MATERIALS AND METHODS

Astrocyte counting in postnatal Bax$^{-/-}$ and WT brains. Bax$^{-/-}$ and wild-type (WT) mice were generated by mating the heterozygous mice, and genotyping was carried out by PCR as described previously (13). Whole-brain tissues at P10 were dissociated, and the brain cells were labeled with glial fibrillary acidic protein (GFAP) antibody (Sigma, St. Louis, MO). The total number of GFAP-labeled astrocytes was determined by flow cytometry analysis as previously described (26), with minor modifications. Whole-brain tissue at P10 was dissociated, and the brain cells were passed through a nylon mesh and suspended in phosphate-buffered saline (PBS). The prepared brain cells were maintained undisturbed at room temperature for 10 min to remove debris, fixed in 2% paraformaldehyde on ice for 20 min, washed, and incubated in 0.5% saponin solution in PBS for 20 min on ice. After being blocked with 1% bovine serum albumin-0.1% saponin in PBS, cells were incubated for 30 min on ice with GFAP antibody (1:400; Sigma). After being washed three times in PBS, the cells were incubated for 30 min with phycoerythrin–anti-mouse immunoglobulin G1 (IgG1) (1:200; BD Biosciences, Franklin Lakes, NJ) and again washed. Stained cells were analyzed with FACSCalibur (BD Biosciences) and CellQuest Pro software (BD Biosciences). A defined fraction of cells was stained with Hoechst33342, and the number was determined using a hemocytometer and fluorescence microscopy. Total astrocyte numbers were calculated based on the percentage of GFAP-positive cells.

Neurosphere culture with neural precursor cells derived from Bax$^{-/-}$ mice. Cerebral cortices were dissected from Bax$^{-/-}$ and WT mouse embryos at E12 and E18. Each tissue was individually subjected to neural precursor cell culture in a separate culture dish with a standard neurosphere culture method (37). Tissue was triturated mechanically in Ca^{2+}-/Mg^{2+}-free Hanks' balanced salt solution (HBSS; Invitrogen, Carlsbad, CA), and resulting cells were seeded in an uncoated 6-cm dish (50,000 viable cells) and cultured in suspension in serum-free defined N2 medium (4) supplemented with B27 (Invitrogen), basic fibroblast growth factor (bFGF; 15 ng/ml; R&D systems, Minneapolis, MN), and epidermal growth factor (EGF; 10 ng/ml; R&D systems). Neural precursor cells were grown for 6 days in the culture medium containing the mitogens bFGF and EGF to generate free-floating cell clusters, also known as the "neurosphere" (reference 16; primary neurosphere). For precursor differentiation, spheres were dissociated mechanically and plated on fibronectin (1 μg/ml; Sigma)-coated 6-cm culture dishes in N2-plus-B27 medium without the mitogens. Differentiation phenotypes were determined after 6 days of culture. In other cases, primary spheres were dissociated into single cells by incubating for 5 h in HBSS followed by mechanical trituration (in this condition, >95% of cells were dissociated into single cells), seeded at a clonal cell density (150 cells/ml/9.6 cm^2) in the medium containing bFGF and EGF, and grown for 3 days to generate the next generation of sphere (secondary spheres). Secondary spheres were directly plated on fibronectin-coated dishes, and differentiation was induced by withdrawing bFGF and EGF. Cultures were maintained in a 5% CO_2 incubator at 37°C and supplemented daily with bFGF and EGF.

Cell culture for rat embryonic cortical precursor cells on fibronectin-coated dishes. For further in vitro analyses, we employed precursor cell culture from rat embryonic cortices, wherein cellular phenotypes are well defined (5). Cells were isolated from rat E14 embryonic cortices as described above and plated at 8,000 cells/cm^2 on fibronectin-coated 6-cm dishes. Cell proliferation was induced with bFGF (15 ng/ml) in N2 medium. Cell clusters, grown on the adherent culture surface, were dissociated at the fourth day of in vitro expansion and replated onto 12-mm glass coverslips (Bellco, Vineland, NJ) or 6-cm culture plates precoated with fibronectin. All experiments were performed on passaged cultures unless specified otherwise. After additional bFGF-dependent expansion, differentiation of the cortical precursors was induced in the absence of bFGF in N2 medium supplemented with B27. For clonal analyses, cells were dissociated into single cells and plated at 2,000 cells per 6-cm dish. After 6 h of settling, isolated cells were marked with a 3-mm circle marker (Nikon, Tokyo, Japan) on the bottom of the plate. Only cells growing within the marked circles were analyzed as clones. Clones were expanded for 6 days and induced to differentiate for 7 days. For conditioned medium experiments, media were conditioned in Bcl-X_L- and Bax-transduced cultures for 48 h, harvested, filtered at 0.22 μm, and maintained at −80°C until use.

Retroviral infection. A reporter retroviral vector, pIRES-GFP, designed for enhanced green fluorescent protein (GFP) expression in infected cells, was constructed by cloning the amplified sequences of the internal ribosomal entry site (IRES) and GFP cDNA into the pCL retroviral vector backbone (detailed information on the vector is available upon request). The human Bcl-X_L fragment (a kind gift of Y.-J. Oh, Yonsei University, South Korea) and mouse Bax cDNA sequences were engineered into pIRES-GFP to generate the expression vectors pBcl-X_L-IRES-GFP and pBax-IRES-GFP, respectively. For mock transduction, the LacZ expression vector pLacZ-IRES-GFP was constructed. Each recombinant plasmid was introduced into the 293gpg retrovirus-packaging cell line by transient transfection, followed by harvesting. For viral transduction, neural precursors cultured in vitro were incubated with the viral supernatant containing Polybrene (hexadimethrine bromide; 1 μg/ml; Sigma) for 2 h, followed by a medium change.

siRNA lentivirus production and transduction. Short interfering RNAs (siRNAs) were transferred using lentiviral vector pLL3.7 (provided by L. van Parijs), which was engineered by introducing the mouse U6 promoter upstream of a cytomegalovirus promoter-based GFP expression cassette to create a vector that simultaneously produces siRNAs and GFP. The sequences used were as follows: mouse Bcl-X_L siRNA, 5′-AAGGAUACAGCUGGAGUCAGU-3′; mouse Bax siRNA, 5′-AACAGAUCAUGAAGACAGGGG-3′ (29). All recombinant lentiviruses were produced by transient transfection of 293FT cells (Invitrogen) following standard protocols (42).

Site-directed mutagenesis. The Bcl-X_L mutants (Y101K and R209stop) and Bax mutants (L63E and T172stop) were constructed by site-directed mutagenesis, using the QuikChange system (Stratagene, La Jolla, CA). The Y101K and L63E mutants code for proteins in which residue 101 (Y) is substituted with K in Bcl-X_L and residue 63 (L) with E in Bax, respectively. The Bcl-X_L mutant, R209stop (Bcl-X_LΔTM), and the Bax mutant, T172stop (BaxΔTM), encode proteins with deletions of 25 and 21 amino acids, respectively, at their C termini.

In utero electroporation. Pregnant ICR mice were provided by Japan SLC (Shizuoka, Japan). At E14, pregnant mice were deeply anesthetized with sodium pentobarbital at 50 μg per gram of body weight, and the uterine horns were exposed. Approximately 2 μl of plasmid solution (2 μg/μl) was injected into the lateral ventricle with a glass micropipette made from a microcapillary tube (GD-1; Narishige, Tokyo, Japan). To monitor the injection procedures, Fast Green solution (1.0%) was added to the plasmid solution at a ratio of 1:20. The embryo in the uterus was placed between the tweezers-type electrode, which has disc electrodes of 5 mm in diameter at the tip (CUY650-5; Tokiwa Science, Fukuoka, Japan). Electronic pulses (35 V; 50 ms) were charged five times at intervals of 950 ms with an electroporator (CUY21E; Tokiwa Science). Electroporated brains were isolated at E18 and P2 and coronally cryosectioned at 15 to 20 μm. Preparation of brain slices for immunohistochemical analyses was carried out as described previously (6). Neuron and astrocyte numbers out of transfected cells were determined for acutely dissociated cortices as previously described (2, 25). Briefly, cortices were dissected and dissociated by serial trituration with 25G-to-30G needles in HBSS. Dissociated cells were seeded on culture dishes precoated with fibronectin (5 μg/ml), followed by overnight settling and postfixation. In this condition, >80% of the dissociated cells or cell clusters were attached to the fibronectin-coated surface. After fixation, immunostaining for neuron and astrocyte makers was performed as follows.

Immunostaining. Cryosectioned brain slices and dissociated or cultured cells were fixed in 4% paraformaldehyde in PBS and incubated with primary antibodies overnight at 4°C. The following primary antibodies were used at the concentrations specified: Ki67 (mouse; 1:200; Novocastra, Newcastle, United Kingdom), nestin (rabbit; 1:50; R. McKay, NIH, Bethesda, MD; or mouse; 1:500; BD Pharmingen), β-tubulin type III (TuJ1) (mouse; 1:500 or rabbit; 1:2,000; both from Covance, Richmond, CA), NeuN (mouse; 1:200; Chemicon, Temecula, CA), GFAP (rabbit; 1:400; DAKO, Glostrup, Denmark; or mouse; 1:100; ICN Biochemicals, Aurora, OH), bromodeoxyuridine (BrdU) (rat; 1:100; Accurate, Westbury, NY), O4 (mouse; 1:500; R&D Systems), GFP (mouse; 1:400; Roche, Basel, Switzerland). Fluorescence (fluorescein isothiocyanate or rhodamine)-labeled secondary antibodies (Jackson ImmunoResearch Laboratories, West Grove, PA) were subsequently applied to detect the binding of the primary antibodies according to the manufacturer's specifications. Cells and tissues were mounted in VECTASHIELD with DAPI (4′-6′-diamidino-2-phenylindole) (Vector Laboratories, Burlingame, CA) mounting medium. Images were ac-

quired on either a Carl Zeiss LMS 510 confocal system (0.5- to 1.0-μm optical sections) or a Nikon Eclipse 400 fluorescence microscope.

Cell viability assays and BrdU incorporation analysis. A terminal deoxynucleotidyltransferase-mediated dUTP-biotin nick end labeling (TUNEL) assay was performed using an in situ cell death detection POD kit (Roche) following the manufacturer's protocol. Cell viability was assessed by the TUNEL assay as well as by directly counting viable cells and clones, as described previously (6). Retrovirally transduced cells were plated at 2,000 cells per 6-cm dish, and viable cells (at day 1) and clones (at day 6 of cell expansion) were counted. For the BrdU assay, cells were pulsed with 10 μM BrdU (Roche) for 0.5 h on the last day of cell expansion, and the incorporation of BrdU was detected using the anti-BrdU antibody as described above.

Immunoblot analyses. Protein samples were electrophoresed in a sodium dodecyl sulfate-polyacrylamide gel electrophoresis gel and transferred to a nitrocellulose membrane, as reported previously (6). Nitrocellulose membrane-transferred proteins were incubated in 5% bovine serum albumin to block nonspecific binding. The blot was probed with an anti-GFAP (mouse; 1:800; ICN Biochemicals; or rabbit; 1:2,500; DAKO), S100 (mouse; 1:2,000; Sigma), TuJ1 (mouse; 1:2,000; Covance), microtubule-associated protein 2 (MAP2) (mouse; 1:2,000; Sigma), Bcl-X_L (rabbit; 1:1,000; Cell Signaling, Inc., Danvers, MA), Bax (rabbit; 1: 1,000, Cell Signaling, Inc.), anti-p44/42 mitogen-activated protein kinase (MAPK) (mouse), phospho-p44/42 MAPK (Thr202/Tyr204; mouse), cyclic AMP response element binding (CREB) protein (rabbit), STAT3 (rabbit), phospho-STAT3 (Tyr705; rabbit), Akt (rabbit), phospho-Akt (Ser473; rabbit) (all at dilutions of 1:1,000; Cell Signaling, Inc.), phospho-CREB (Ser133; rabbit; 1:500; Affinity BioReagents, Golden, CO), or β-actin (mouse; 1:2,000; Sigma) followed by peroxidase-conjugated anti-rabbit IgG (New England Biolabs, Inc., Beverly, MA) or anti-mouse IgG (New England Biolabs) at 1:2,000 dilution. Bands were visualized by enhanced chemiluminescence (ECL detection kit; Amersham-Pharmacia Co., Buckinghamshire, United Kingdom). Signals were quantified by scanning films with Quantity One 1-D Analysis (background subtraction method [local background]; version 4.3.1; Bio-Rad, Hercules, CA).

Reverse transcription-PCR analysis. Transduced cells were cultured in the presence of bFGF for 2 days and subjected to reverse transcription-PCR analysis. RNA extraction, mRNA reverse transcription, and PCR analysis were performed using standard protocols (6). The following primer sequences and PCR conditions were used: Id1, TGAACGTTCTGCTCTACGACA and AGAGGCATTC CCACTTCTCTA; Id2, TGACGTCCGTTAGGAAAAACA and GAAAAAGT CCCCAAATGC; and Id3, AACCTCCAACATGAAGGCG and AGTTCAGT CCTTCGCTCTCG (56°C with 2 mM $MgCl_2$). PCR conditions for other genes were similar to those reported earlier (4). PCR products were separated on a 1.0% agarose gel, followed by ethidium bromide staining. Real-time PCR was performed on an iCycler iQ (Bio-Rad) using SYBR (Molecular Probes, Eugene, OR), and each gene was quantified as described previously (6).

Statistical analysis. Cell counting was performed for randomly chosen microscopic fields by use of an eyepiece grid at a final magnification of ×200 or ×400. Statistical comparisons were performed using SPSS software (version 11.0; SPSS Inc., Chicago, IL). One-way analysis of variance (ANOVA) was applied. All results are presented as means ± standard errors of the means (SEM), and the null hypothesis was rejected on the basis of P values of <0.05.

RESULTS

Decreased astrocyte formation in Bax-KO mice. Bcl-X_L knockout (Bcl-X_L-KO; Bcl-$X_L^{-/-}$) mice are prone to early death, succumbing to a massive loss of neurons in the brain (21), which presumably occurs due to the apoptosis of cells in neuronal lineage and/or a defect in neuron formation. In contrast, Bax knockout (Bax-KO) mice are viable but show increased neuronal populations in neuromuscular junctions (31) and hippocampal dentate gyrus (32). Since no study has yet closely examined the effect of Bax on the development of astrocytes, we first examined whether astrocyte formation is influenced by Bax deletion.

Surprisingly, the expression of GFAP and S100β, the markers for astrocytes, was significantly decreased in the cortices of $Bax^{-/-}$ mice at P2, the peak period of astrocyte formation, and at P14, the time point by which astrocyte formation is terminated (23). In contrast, the expression of neuronal markers MAP2 and TuJ1 showed a clear increase in the cortices of Bax-KO mice at these perinatal ages (Fig. 1a and b). We attempted to compare astrocyte numbers between normal WT and Bax-KO mouse cortices but were unable to count $GFAP^+$ cell numbers accurately in the developing brain, as the $GFAP^+$ cell counts varied significantly among sectioned slices. This was most likely due to the scattered spatial dispersion of colonies of newborn astrocytes in the developing brain (22, 41), in contrast to cortical neurogenesis taking place during the embryonic stage with a systematic laminar colonization of postmitotic neurons. Therefore, to assess the number of astrocytes in Bax-KO and WT embryonic brains, we dissociated the whole brain at P10 into single cells, labeled glial cells fluorescently with GFAP antibody, and quantified the number of GFAP-labeled astrocytes by flow cytometry (Fig. 1c). Quantification of total cell numbers from Bax-KO and WT P10 brains revealed no significant difference (for Bax-KO, $5.3 \times 10^7 \pm 0.3 \times 10^7$ cells [$n = 4$], and for WT, $5.1 \times 10^7 \pm 0.1 \times 10^7$ cells [$n = 6$], in three independent experiments; $P = 0.926$), suggesting that Bax-dependent cell death does not significantly affect the total number of brain cells at this stage. On the other hand, we observed a smaller proportion of cells being GFAP-labeled astrocytic cells for Bax-KO mice than for WT littermates (29.4% ± 2.0% versus 35.9% ± 1.3%). The total number of astrocytes per brain estimated based on this observation indicated a substantial and significant reduction of $GFAP^+$ astrocytes in Bax-KO mice compared to what was seen for WT littermates: $1.4 \times 10^7 \pm 0.2 \times 10^7$ cells for Bax-KO ($n = 4$) versus $1.8 \times 10^7 \pm 0.4 \times 10^7$ cells for WT ($n = 6$) ($P < 0.05$) (Fig. 1d). The difference in the numbers of $GFAP^+$ cells became insignificant past the postnatal age of 1 month (data not shown), suggesting that a compensatory gliogenic mechanism promoting astrocyte formation comes into play at some point.

Astrogenic potential of cortical precursors isolated from Bax-KO embryos. We sought to determine the differentiation potentials of neural precursor cells isolated from Bax-KO and WT mouse embryos. Cortices at E12 and E18 were dissociated, and neural precursor cells were selectively proliferated in vitro as "neurospheres" by applying bFGF and EGF, the mitogens for neural precursors.

The number of viable cells or spheres in $Bax^{-/-}$ cultures was greater than that in WT cultures by 40 to 60%. To minimize the influence of cell survival effect on precursor differentiation, pan-caspase inhibitor z-VAD-FMK (20 μM) was added in all the cultures, and this rendered cell survival indices for the WT and $Bax^{-/-}$ cultures essentially indistinguishable (effects of z-VAD-FMK on cell survival are further described in the following section). The neurospheres were plated on fibronectin-coated plates and were induced to differentiate by withdrawing the mitogens. Total cell numbers of the z-VAD-FMK-treated WT (1,964 ± 66 cells/well) and Bax-KO cultures (1,957 ± 178 cells/well) were not significantly different. In the differentiation conditions of WT cultures, 41.4% ± 5.5% (811 ± 123 cells/well) and 47.4% ± 5.4% (924 ± 111 cells/well) of the cells were positive for GFAP and TuJ1, respectively. Significantly fewer $GFAP^+$ cells (30.7% ± 2.8%; 592 ± 77 cells/well) and more $TuJ1^+$ neurons (55.8% ± 3.3%; 1,094 ± 81 cells/well) than for the WT cultures were observed for the differentiated cultures of Bax-KO precursors (Fig. 2a, left; percentages of neurons and astrocytes were significantly different at P values of

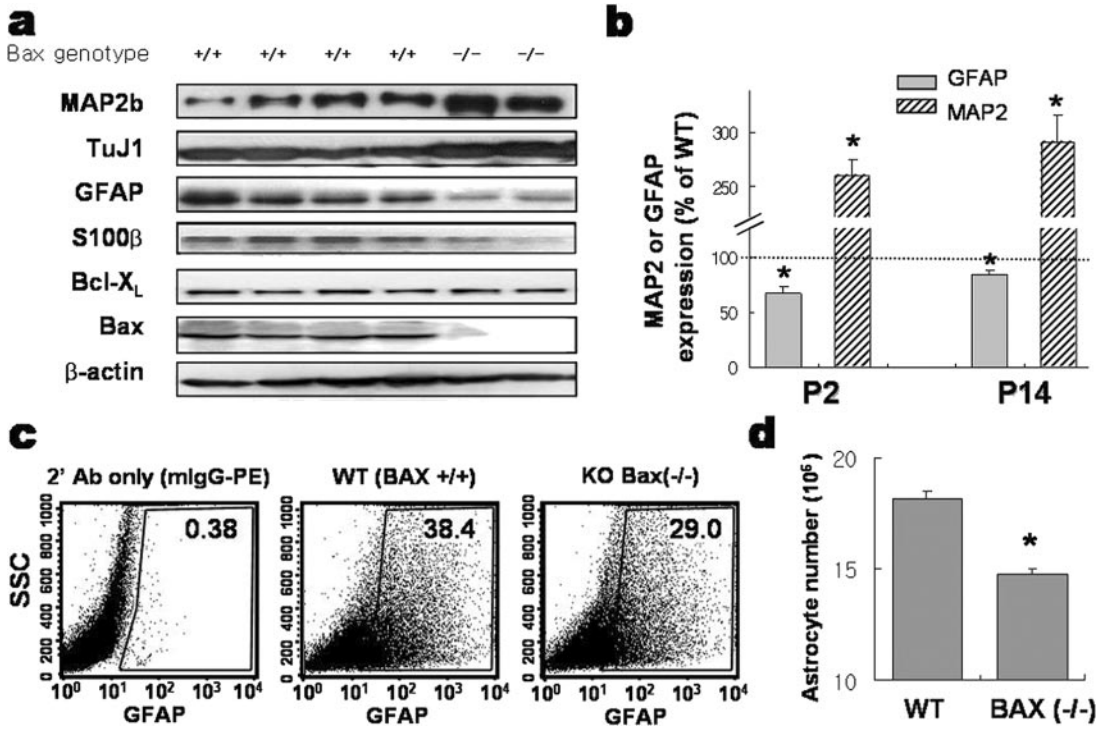

FIG. 1. Reduced formation of astrocytes in the developing cortex of Bax-KO mouse. Cerebral hemispheres were dissected from WT and Bax-KO mice at P2 and P14 and were subjected to immunoblot analyses for expression of astrocytic markers GFAP and S100β and neuronal markers TuJ1 and MAP2. (a) Representative immunoblots of WT and Bax-KO cortices at P2 are shown. (b) Each GFAP and MAP2 band of WT and Bax-KO animals was scanned for quantification. The data were obtained from the P2 offspring ($n = 4$ for Bax-KO and $n = 9$ for WT) from three pregnant mice and from P14 offspring ($n = 3$ for Bax-KO and $n = 5$ for WT) from two pregnant animals. *, significantly different from WT control at a P value of <0.001. (c and d) Reduction in the number of GFAP-positive astrocytes in Bax-KO brain. Brain cell suspensions from P10 mice were fixed, permeabilized, and immunostained with anti-GFAP antibody (Ab). The percentage of GFAP-labeled cells was obtained by a flow cytometer. Shown in panel c are representative profiles of the flow cytometry analyses. The boxed area includes the GFAP-labeled cells recognized and separated on the basis of secondary antibody fluorescence emission pattern. SSC, side scatter. The number of astrocytes per brain, as shown in panel d, was calculated by multiplying the astrocyte ratio by the total cell number in the brain. Means ± SEM of six (WT) or four (Bax-KO) animals were from three independent experiments. *, $P < 0.05$ in Student's t test comparison.

<0.001). Similar expression patterns of GFAP and TuJ1 were demonstrated by the immunoblot analyses for the protein levels in the differentiated cultures of the Bax-KO and WT precursors (Fig. 2a, middle and right). A reduced astrocyte production, along with an enhanced yield of neurons, was similarly observed for E18 precursor cultures by Bax deletion (Fig. 2b).

Primary neurospheres were dissociated into single cells and plated at a clonal cell density (150 cells/ml/9.6 cm^2) in the medium containing bFGF plus EGF to obtain the next generation of spheres (secondary spheres). Virtually all spheres are clonally derived at this plating density (28, 33). With z-VAD-FMK treatment, out of 5,000 dissociated single cells, 279 ± 31 and 303 ± 26 spheres were formed in the WT and Bax-KO cultures, respectively. The resultant secondary spheres were allowed to differentiate in the absence of the mitogens to examine their differentiation phenotypes. As shown in Fig. 2c, in the E12 WT cultures, 21.2% ± 3.4%, 5.8% ± 1.1%, and 59.4% ± 3.2% of secondary spheres differentiated into colonies containing astrocytes only, neurons only, and mixed neurons and astrocytes, respectively. In contrast, the percentage of astrocyte-only spheres (9.9% ± 3.6%) was significantly less and the percentage of neuron-only spheres (15.7% ± 2.9%) was significantly greater in the cultures from E12 Bax-KO mice. In E18 cultures, the majority of secondary spheres isolated from WT embryonic cortices were astrocyte-only spheres (79.9% ± 1.3%). The spheres containing both neurons and astrocytes were in the minority (13.2% ± 1.7%), and none of the spheres contained neurons only (Fig. 2d). This is consistent with the dominant gliogenic potential of neural precursors in late developmental stages (for a review, see reference 23). The cultures from E18 Bax-KO mice, in contrast, contained a markedly greater number of bipotent neuron-plus-astrocyte spheres (63.3% ± 5.0%) at the expense of astrocyte-only spheres (29.5% ± 3.8%). These findings, taken together, suggest that Bax may be responsible for the neurogenic-to-astrogenic transition of the precursor differentiation potential.

Bcl-X_L and Bax direct cortical precursor cells to differentiate into neurons and astrocytes, respectively. In order to further define the role of Bax in astrocytic formation and to extend the study to Bcl-X_L, which has a role opposite to that of Bax in the regulation of cell death, gene manipulation of Bax and Bcl-X_L was performed in the cultures of embryonic cortical precursors. We previously demonstrated that a homogeneous population of undifferentiated neural precursor cells could be obtained from rat embryonic cortex by in vitro proliferation of the precursors and mechanical elimination

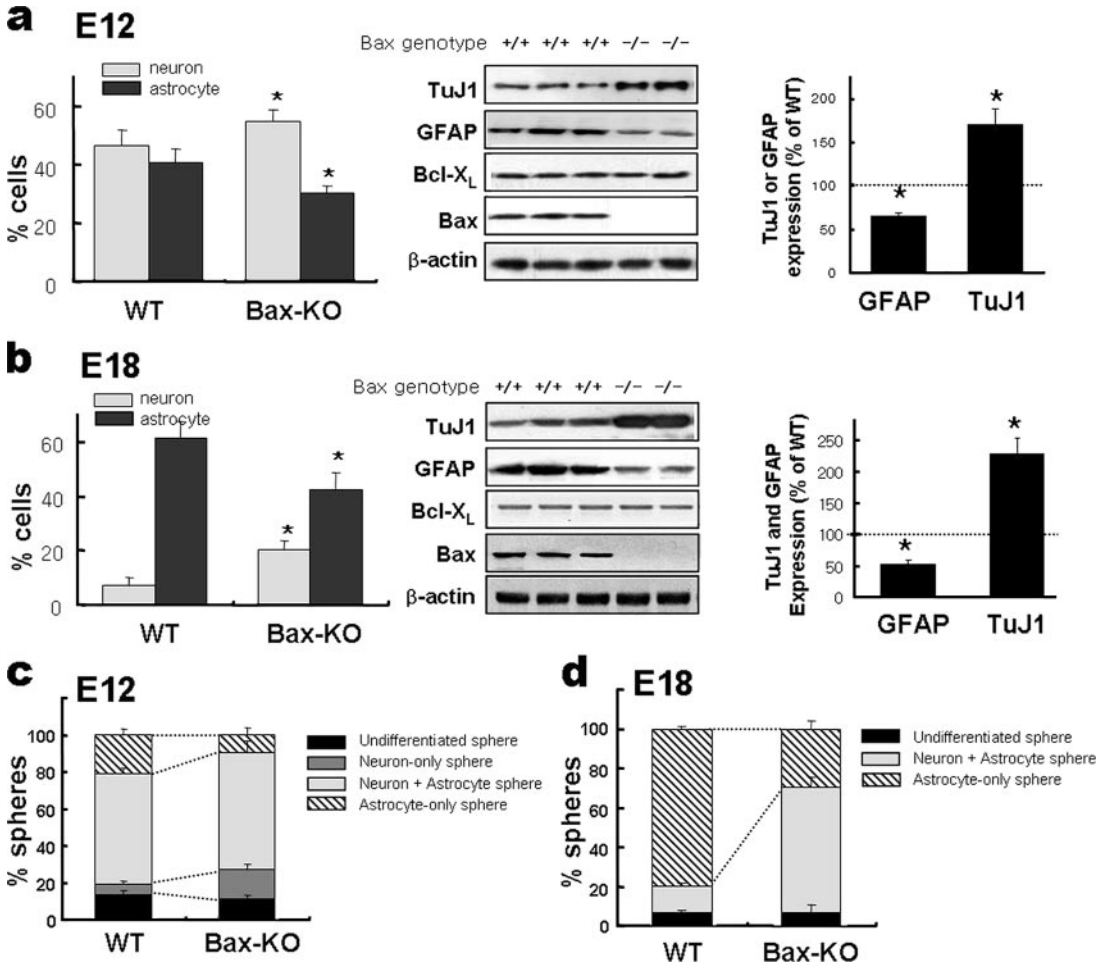

FIG. 2. In vitro differentiation potential of the precursor cells derived from Bax-KO embryonic cortices. Neural precursor cells were isolated from WT and Bax-KO embryonic cortices at E12 (a and c) and E18 (b and d) and cultured in suspension to generate floating spheres (primary spheres) as described in Materials and Methods. The yields of neurons and astrocytes under the differentiation condition were estimated by counting $GFAP^+$ astrocytes and $TuJ1^+$ neurons (left panels of a and b) as well as by determining the expression level of these markers (middle and right panels of a and b). The immunoblot bands were scanned for quantification (right panels of a and b). (c and d) Differentiation phenotype of clonally derived secondary spheres. Differentiation potentials of the spheres were assessed after in vitro differentiation based on the numbers of spheres containing neurons only, astrocytes only, and mixed populations of neurons and astrocytes. The data were obtained from 7 WT and 4 Bax-KO E12 embryos and 14 WT and 6 Bax-KO E18 embryos. All the cultures were performed in the presence of pancaspase inhibitor z-VAD-FMK. *, $P < 0.001$.

of differentiated or differentiating cells through the passaging procedure (5). Over 95% of thus prepared rat E14 cortical precursor cells were positive for nestin when expanded in vitro for 4 days with bFGF (see Materials and Methods).

$Nestin^+$ precursor cells readily differentiated into neurons and astrocytes by withdrawal of bFGF: 35.9% ± 5.4% and 26.7% ± 2.3% of cells were positive for TuJ1 and GFAP, respectively, 6 days after bFGF withdrawal. Oligodendroglial differentiation, estimated by the number of cells positive for the oligodendrocyte marker O4, was relatively minor (percentage of $O4^+$ cells, 6.8% ± 0.8%). A fraction of the cells (21.7% ± 1.8%) remained as undifferentiated $nestin^+$ cells after 6 days.

To examine whether the neuron-astrocyte differentiation potentials of neural precursors can be altered by elevated levels of Bcl-X_L or Bax, precursor cells isolated from rat E14 cortices were transduced with pBcl-X_L-IRES-GFP, pBax-IRES-GFP, and pLacZ-IRES-GFP (control) retroviral vectors (see Materials and Methods). Retroviral gene transfer, as estimated by the expression of GFP 2 days after the infection, was found to be efficient and indistinguishable among the three vectors. Specifically, GFP^+ cells were 92.2% ± 1.4%, 90.4% ± 0.5%, and 91.3% ± 1.8% of total cells in cultures transduced with Bcl-X_L, Bax, and LacZ vectors, respectively ($n = 16$ for each value). The anti-/proapoptotic effects of Bcl-X_L/Bax were examined for the precursor cells by TUNEL assay and direct counting of viable cells in cultures plated at a clonal density (see Fig. S1a and b in the supplemental material). It was shown that Bcl-X_L/Bax overexpression did not alter cell proliferation indices, including the percentage of Ki67-positive cells (see Fig. S2 in the supplemental material). Specifically, percentages of $Ki67^+$ cells were 27.1% ± 2.5%, 29.5% ± 1.6%, and 23.3% ± 1.7% of total cells in cultures transduced with LacZ (control)-, Bcl-X_L-, and Bax-expressing vectors, respectively, at

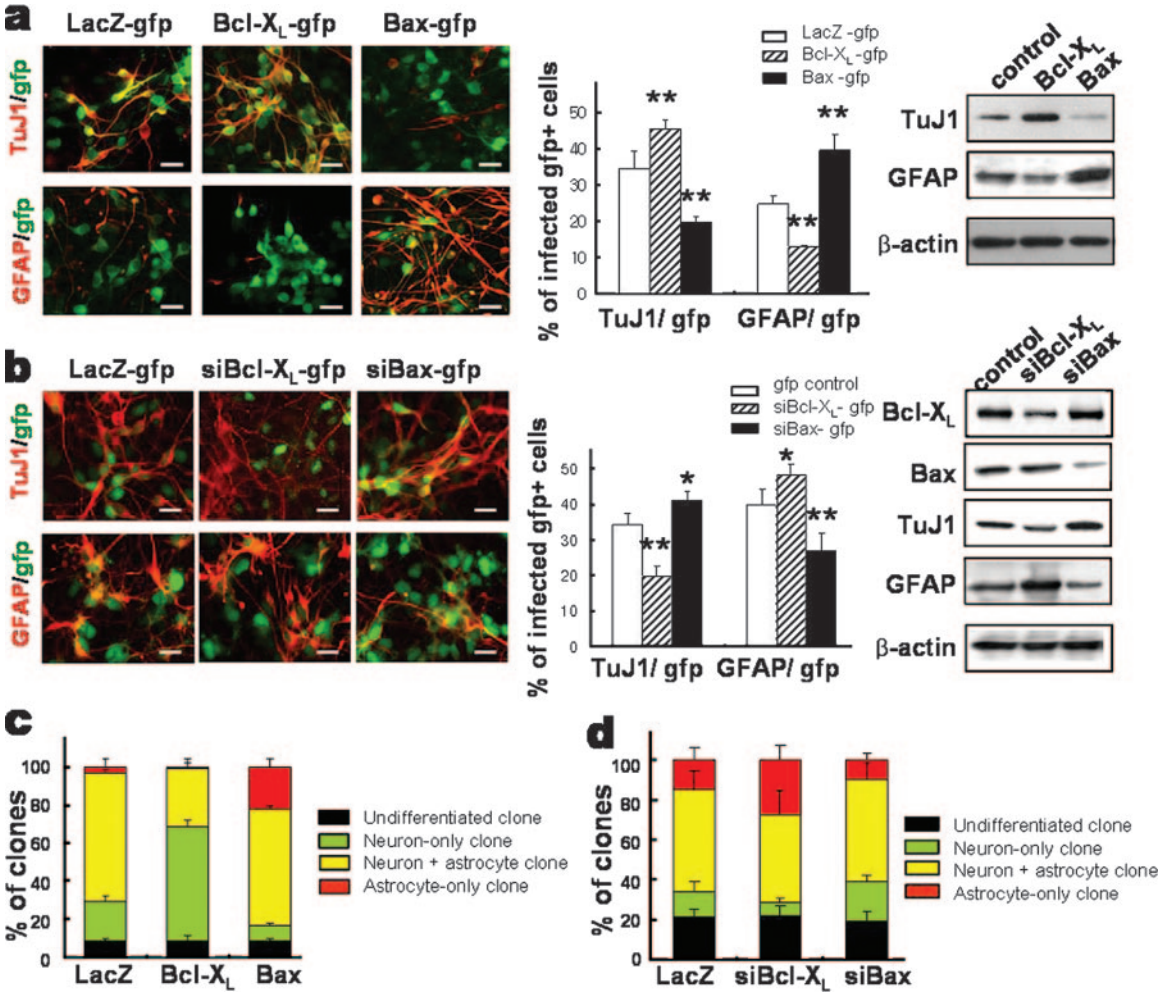

FIG. 3. Gain- and loss-of-function experiments for Bcl-X_L and Bax with neural precursor cells in vitro. Neural precursors from rat E14 cortices were infected with viruses encoding LacZ-gfp (control), Bcl-X_L-gfp and Bax-gfp (a and c), or siBcl-X_L-gfp and siBax-gfp (b and d). The effects of overexpression (a and c) and silencing (b and d) of Bcl-X_L and Bax on precursor differentiation were determined by immunocytochemical (left and middle in panels a and b) and immunoblot (right in panels a and b) analyses for TuJ1 and GFAP. Representative images of the immunostaining are shown at left in panels a and b. Graphs in the middles of panels a and b show the percents TuJ1$^+$ neurons and GFAP$^+$ astrocytes out of total infected cells (GFP$^+$ cells). Lineage analysis of clones derived from single isolated precursor cells are shown in panels c and d. Cells infected with Bcl-X_L-gfp or Bax-gfp (c) or siBcl-X_L-gfp or siBax-gfp (d) were plated at a clonal density, and in vitro proliferation into clones followed. Differentiation phenotypes of GFP$^+$ clones were assessed by staining for TuJ1 and GFAP and counting the numbers of neuron-only, neuron-plus-astrocyte, astrocyte-only, and undifferentiated clones. Each value represents mean ± SEM (n = 16 to 24 microscopic fields from three to four independent experiments). The experiments were performed in the presence of z-VAD-FMK. *, $P < 0.05$; **, $P < 0.001$ (compared with the value of each mock control-transduced culture; ANOVA). Scale bars, 20 μm.

the last day of differentiation. Tukey post hoc analysis of one-way ANOVA indicated that such results do not represent significant differences.

Differentiation of the transduced precursors was induced by withdrawing bFGF, and the effects of Bcl-X_L/Bax on precursor differentiation were examined at day 6 of differentiation. In the differentiated cultures supplemented with the caspase inhibitor, total cell numbers were not significantly different among the groups: 3,336.0 ± 349.8 (control), 3,759.5 ± 333.5 (Bcl-X_L), and 3,185.7 ± 415.4 (Bax) cells/mm^2. Compared to what was seen for LacZ-transduced control cultures, a significantly greater number of cells was positive for the neuronal marker TuJ1 in differentiated Bcl-X_L-transduced cultures (Fig. 3a). The increase in the number of TuJ1$^+$ cells was accompanied by a decrease in the number of GFAP$^+$ astrocytes. Conversely, the extent of astrocyte formation from Bax-transduced cultures was greater than that from control cultures at the cost of reduced neurogenesis (Fig. 3a) (TuJ1$^+$ neurons/mm^2, 1,172.1 ± 227.7 [control], 1,758.8 ± 366.4 [Bcl-X_L], and 573.7 ± 92.0 [Bax]; GFAP$^+$ astrocytes, 778.6 ± 57.7 [control], 459.0 ± 103.3 [Bcl-X_L], and 1,128.4 ± 82.1 [Bax]; significantly different from the control values of neurons and astrocytes at P values of <0.001; n = 72 from six independent experiments for each value). It is noted that the fractions of differentiated cells (percent TuJ$^+$ neurons plus percent GFAP$^+$ astrocytes) out of total cells were not significantly different among the three groups (59.1% versus 58.0% versus 59.2%), indicating that the cell fate switches but not the overall differentiation was induced by the Bcl-2 family proteins.

Apoptotic cell death induced by Bcl-2 family proteins is

mediated through the activation of caspase proteins (30, 40). In the present study, pan-caspase inhibitors z-VAD-FMK (20 μM [30]) and Boc-D-FMK (20 μM [8]) maintained the cell survival in LacZ- and Bax-transduced cultures up to the point where cells were infected with Bcl-X_L. Consequently, no significant differences in the cell viability indices were observed among these culture groups (see Fig. S1 in the supplemental material). Furthermore, the enhancement of cell survival following the addition of caspase inhibitors was not accompanied by significant alterations in neuronal and astrocytic yields (for example, in Bax-transduced cultures, neuronal numbers in the presence versus the absence of z-VAD-FMK were 19.7% ± 1.2% versus 21.1% ± 0.4% [$P = 0.35$], while astrocytic numbers were 39.5% ± 4.5% versus 43.9% ± 1.6% [$P = 0.41$]). These findings suggest that Bcl-X_L/Bax-mediated precursor differentiation is separable from the survival and death effects. In order to be independent of Bcl-X_L/Bax-mediated anti-/pro-apoptotic effects, all the experiments for precursor cell differentiation in this study were performed in the presence of z-VAD-FMK unless otherwise noted.

For further confirmation of the roles of Bcl-X_L/Bax in the precursor differentiation, we carried out loss-of-function experiments via gene silencing with siRNA. Infection efficiencies of lentiviral preparations used for siRNA transfers were 43 to 51%, without significant variations among Bcl-X_L, Bax, and control siRNA vectors, as assessed by GFP expression. siRNAs against Bcl-X_L and Bax were effective in reducing the endogenous levels of Bcl-X_L and Bax, respectively (Fig. 3b, right). Silencing of Bcl-X_L resulted in an increase of astrocytic yield at the expense of neuron formation, whereas a change in opposite direction was observed for the cultures infected with Bax siRNA (Fig. 3b). These results further confirm that Bcl-X_L and Bax induce differentiation of the cortical precursor cells into neuronal and astrocytic lineages, respectively (Fig. 3c).

Bcl-X_L/Bax instructively direct the cell fate specification of neural precursors. The number of $TuJ1^+$ neurons and $GFAP^+$ astrocytes gradually increased after bFGF withdrawal. Increases in neurons and astrocytes by Bcl-X_L and Bax overexpression were observed from the beginning of the differentiation induction. Only 1 day after bFGF withdrawal, the percentage of $TuJ1^+$ neurons in Bcl-X_L-transduced cultures was significantly higher (2.4% ± 0.5% [$P < 0.05$]) than that in control cultures (0.7% ± 0.2%). Also, while none of the cells were positive for GFAP in the LacZ control- and Bcl-X_L-transduced cultures at day 1 of differentiation, 0.15% of Bax-transduced cells were positive for GFAP. To label neuronal and astrocytic progenitors (the term "progenitors" in this study is assigned to the committed precursor cells whose fate is determined), cells were pulsed with BrdU for 0.5 h on the last day of expansion, and the percentages of BrdU/TuJ1 (neuronal progenitor) and BrdU/GFAP (astrocytic progenitor) double-positive cells out of total $BrdU^+$ cells were determined at day 7 of differentiation (4, 6, 34). Compared to what was seen for control cultures, the percentage of neuronal progenitors was greater in Bcl-X_L-overexpressed cultures, while a higher proportion of astrocytic progenitors was observed for Bax-overexpressed cultures (see Fig. S3 in the supplemental material).

Treatment with conditioned medium from Bcl-X_L- or Bax-transduced cultures did not affect the precursor cell differentiation (data not shown), ruling out the possibility that Bcl-X_L/Bax-induced precursor differentiation is indirectly mediated via diffusible secreted factors.

In order to confirm that the fate specification induced in cortical precursor cells by Bcl-X_L and Bax occurs in a cell-autonomous manner, we carried out lineage analyses of single cells. Precursor cells transduced with Bcl-X_L/Bax or Bcl-X_L/Bax siRNAs were plated at a clonal density, and differentiation phenotypes of clonally derived clusters (clones) were determined. The average numbers of clones formed (clones/dish) were 49.7 ± 1.4, 48.2 ± 3.4, and 48.1 ± 0.7 in the cultures transduced with LacZ control, Bcl-X_L, and Bax, respectively. Of LacZ-transduced control clones, 21.0%, 2.9%, and 67.3% were neuron only, astrocyte only, and mixed (neuron plus astrocyte), respectively. For Bcl-X_L-infected cultures, we observed a significant increase in neuron-only clones (60.5%) at the expense of astrocyte-only (1.4%) and mixed (30.7%) clones compared to control cultures (Fig. 3c). On the other hand, in cultures transduced with Bax, a reverse situation, wherein the number of astrocyte-only clones increased at the expense of neuron-only clones, was observed. Specifically, 8.1%, 21.8%, and 61.6% were neuron-only, astrocyte-only, and mixed clones, respectively. Furthermore, clonal analyses using cells transduced with Bcl-X_L/Bax siRNAs demonstrated that neuron-to-astrocyte and astrocyte-to-neuron shifts occur upon knockdown of Bcl-X_L and Bax, respectively (Fig. 3d). These findings collectively demonstrate that the instructive effect of Bcl-X_L/Bax proteins in the cell fate specification of neural precursors occurs in a cell-autonomous manner.

Dimerization and mitochondrial localization are not required for the roles of Bcl-X_L/Bax in precursor differentiation. The regulatory functions of Bcl-2 family proteins in cell apoptosis depend on homo- or heterodimerization and subcellular localization to mitochondria (9). The Bax inhibitor V5 is a cell-permeable peptide that imparts its inhibitory effect by physically interacting with the C terminus of Bax in the cytosol and preventing mitochondrial localization of the protein (24). In the present study, Bax-mediated apoptosis in E14 cortical precursor cultures was prevented by V5. Specifically, a significant decrease in the percentage of $TUNEL^+$ cells was observed for V5 (100 μM) treatment of the Bax-transduced cultures (in the absence of z-VAD-FMK, 20.8% ± 0.8% for V5-treated versus 29.0% ± 1.3% for untreated cultures at day 3 of cell proliferation; $n = 16$; $P < 0.001$). However, V5 treatment did not significantly alter Bax-induced astrocytic differentiation: astrocytes accounted for 39.1% ± 1.1% (V5 treated) versus 39.5% ± 3.0% (untreated) ($P = 0.98$) and neurons accounted for 20.0% ± 1.3% versus 19.1% ± 1.4% ($P = 0.32$) of the cells in differentiated cultures.

Mutagenesis studies have revealed that the BH3 domain, in particular the Y101 residue in Bcl-X_L (20) and the L63 residue in Bax (36), is critical for dimerization, while the C-terminal tail plays a critical role in mitochondrial localization (38). In cultures of precursor cells transduced with Bcl-X_L mutants for dimerization (Y101K) and for C-terminal truncation (R209stop, Bcl-X_LΔTM), $TUNEL^+$ cell numbers were significantly greater than those for cultures transduced with WT Bcl-X_L (Fig. 4b). In contrast, these mutations did not affect Bcl-X_L-induced neuronal differentiation (Fig. 4c). Similarly, while substitution of L63 with E (L63E) and truncation of the C-terminal tail in Bax (T172stop, BaxΔTM) abolished the pro-

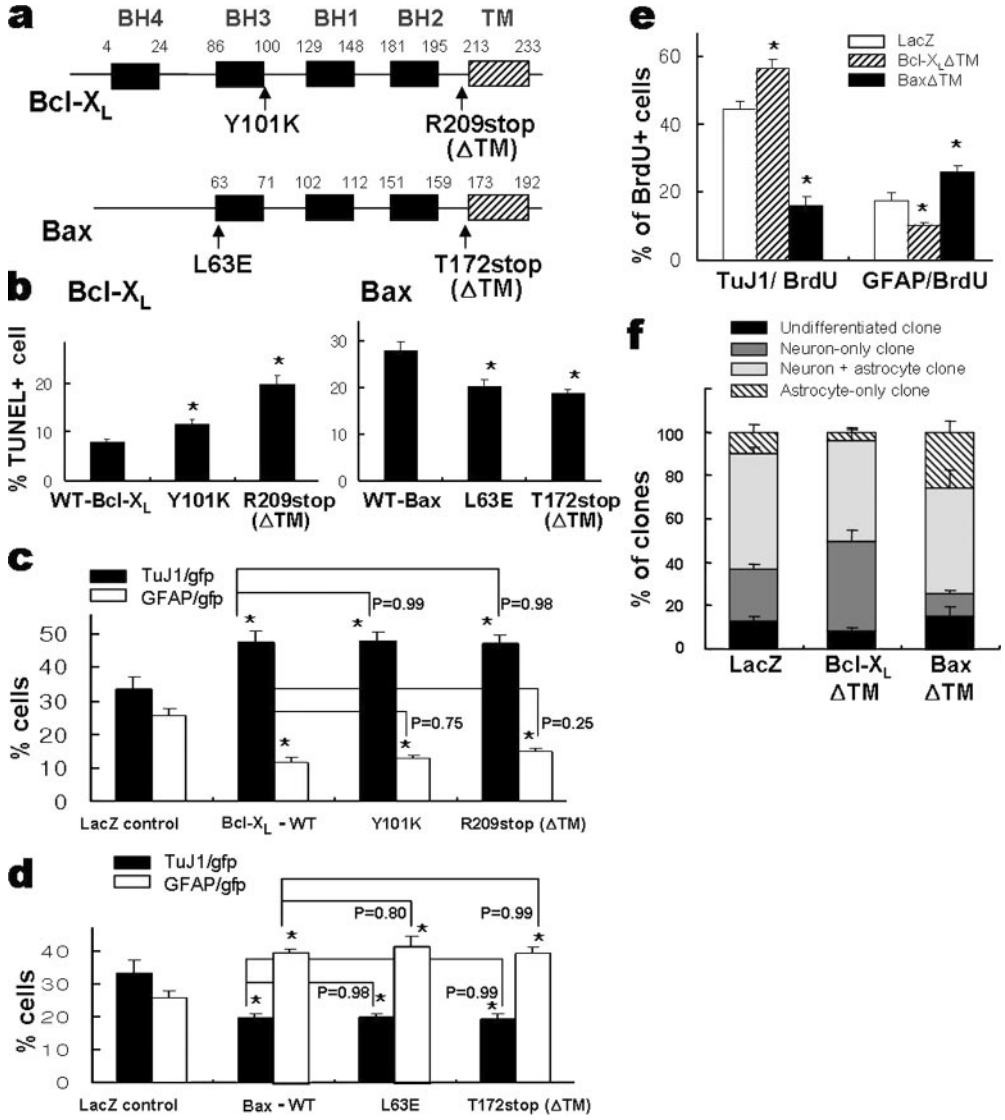

FIG. 4. Dimerization and mitochondrial localization are not required for Bcl-X_L/Bax-induced neuronal/astrocytic differentiation. (a) Schematic representation of the different mutants tested with the common Bcl-X_L and Bax domains in boxes. Site-directed mutagenesis was performed in the BH3 domains (Y101K and L63E) and C-terminal tails (R209stop and T172stop) required for dimerization and mitochondrial localization of the Bcl-2 protein family. Cultured precursors were transduced with mutant vectors. Two days after transduction, cell differentiation was induced for 6 days. Effects of the mutations on cell apoptosis and differentiation of precursor cells were examined using the TUNEL assay (b) and immunocytochemical detection of $TuJ1^+$ neurons and $GFAP^+$ astrocytes (c and d). The TUNEL and immunochemical assays were performed 2 and 8 days after transduction, respectively. Note that the mutations significantly altered precursor apoptosis but not the differentiation properties of Bcl-X_L and Bax proteins. (e) Percentages of committed neuronal and astrocytic progenitors. To label committed neuronal and astrocytic progenitors, cells transduced with Bcl-X_LΔTM or BaxΔTM were pulsed with 10 μM BrdU for 0.5 h, as described in the text. After 7 days of in vitro differentiation, immunostaining was done either for BrdU and TuJ1 or for BrdU and GFAP. The percentages of cells doubly positive for BrdU/TuJ1 (neuronal progenitor) and BrdU/GFAP (astrocytic progenitor) out of total $BrdU^+$ cells are depicted. (f) Lineage analysis of the clones derived from Bcl-X_LΔTM/BaxΔTM-transduced precursors. Clonal analyses were performed as described for Fig. 3c. Note that the effects of the truncation mutants of Bcl-X_L and Bax in committed progenitor pools and clonal phenotypes are indistinguishable from those of WT, as shown in Fig. 3c. *, $P < 0.001$, compared with the value of WT (b) or LacZ-expressing control (c, d, and e). *P* values were analyzed by comparing each WT Bcl-X_L- or Bax-transduced culture by ANOVA.

apoptotic effect of Bax (Fig. 4b), the mutants retained their astrogenic function (Fig. 4d). In addition, committed progenitor cell populations (Fig. 4e) and differentiation phenotypes of the clones (Fig. 4f) derived from the cells transduced with Bcl-X_LΔTM and BaxΔTM mutants were similar to those of their respective full-length WTs. These findings collectively suggest that dimerization and mitochondrial localization are not critical for Bcl-X_L/Bax-induced precursor differentiation and provide additional evidence for the functional separation between precursor differentiation and regulation of apoptosis elicited by the Bcl-2 family proteins.

To determine if the Bcl-2 proteins show similar effects in differentiation of neural precursor cells during development in vivo and if such activities are independent of their functions

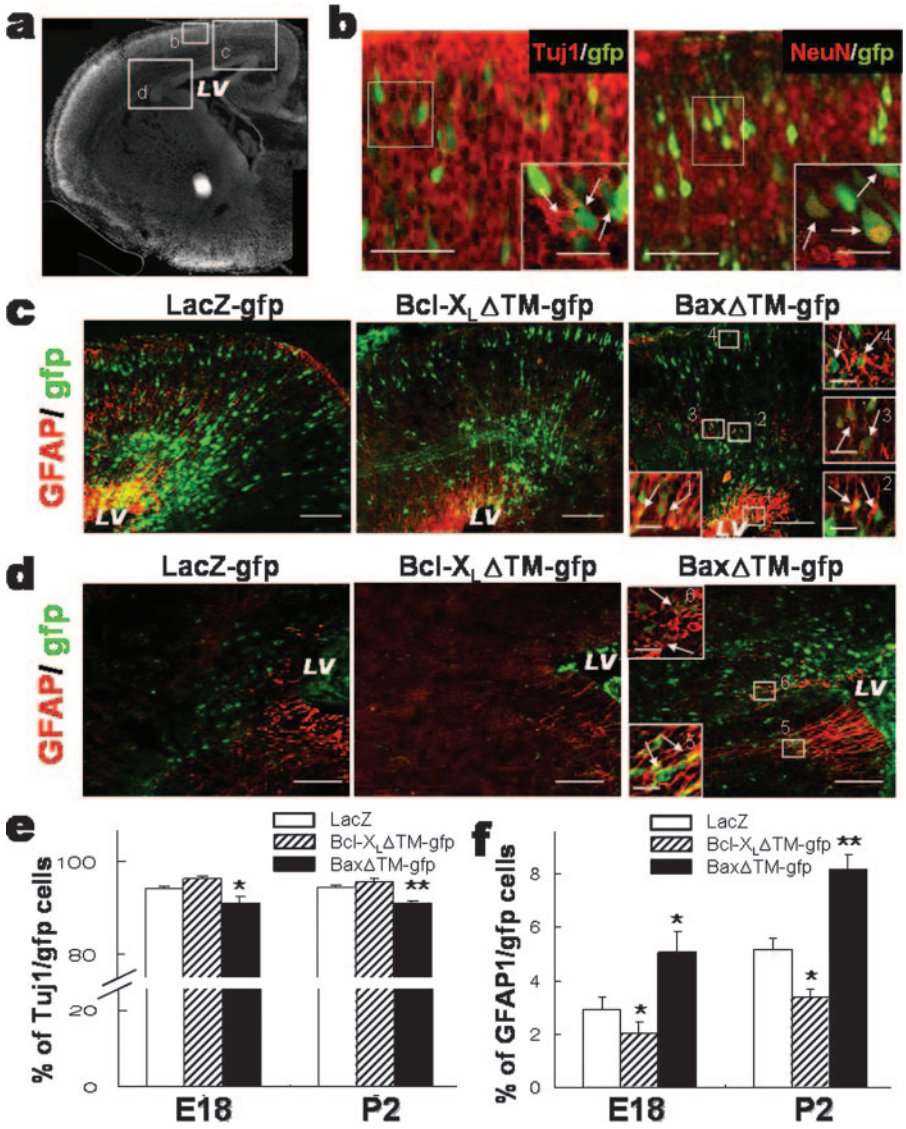

FIG. 5. In vivo differentiation and distribution of cortical precursor cells transfected with gfp-Bcl-X_LΔTM, and gfp-BaxΔTM. Neural precursor cells lining the lateral ventricle (*LV*) of E14 cortex were transfected with gfp-Bcl-X_LΔTM, gfp-BaxΔTM, and the gfp-LacZ control by in utero electroporation, and the distribution and differentiation of transfected (GFP^+) precursors were subsequently analyzed at E18 and P2. (a) A coronal section of E18 cortical hemisphere stained with DAPI nuclear staining. (b to d) Images were captured from the specified boxed areas in panel a. All the images were taken from similar levels of coronal sections. (b) Colocalization of neuronal markers TuJ1 (left) and NeuN (right) in radially migrated GFP^+ cells of the gfp-LacZ-transfected control brain. Insets, high-magnification views of the boxed regions. Scale bars: 50 μm; 20 μm for insets. (c and d) Representative images of GFAP/gfp-stained sections. Note that a relatively higher proportion of GFP^+ cells in Bax-transfected brains is seen in area d, where early glial progenitors migrating mediolaterally are usually detected (32). Scale bars: 100 μm; 20 μm for insets. TuJ1/gfp-, NeuN/gfp-, and GFAP/gfp-colabeled cells are indicated by arrows. (e and f) Percentages of TuJ1/gfp (e) and GFAP/gfp (f) double-labeled cells out of total GFP^+ cells. Each cortex was dissected and dissociated as described in Materials and Methods. The dissociated cortices were attached on fibronectin-coated plates and followed by TuJ1/gfp and GFAP/gfp immunostaining. Proportions are significantly different from those for the gfp-LacZ control at *P* values of <0.05 (*) and <0.001 (**) (n = 79 to 168 microscopic fields from three to six embryos).

in the regulation of apoptosis as seen in vitro, bicistronic GFP reporter vectors carrying Bcl-X_LΔTM (pBcl-X_LΔTM-IRES-GFP) or BaxΔTM (pBaxΔTM-IRES-GFP) mutant genes were introduced into the developing mouse lateral ventricle at E14 by use of an in utero electroporation technique. The differentiation phenotypes of GFP-labeled cells were subsequently analyzed at E18 and P2 (Fig. 5e and f). A clear difference in the distribution of GFP^+ transfected cells was observed between E18 brains transfected with BaxΔTM and those transfected with the control or Bcl-X_LΔTM. Most of the GFP^+ cells in control and Bcl-X_LΔTM-transfected brains were localized in the cortical plates adjacent to the lateral ventricles where the vector DNAs were injected (Fig. 5c). Over 90% of the GFP-expressing cells were positive for TuJ1, consistent with radial migration and neurogenic potential, two well-established characteristics of the precursors found in the ventricular or subventricular zones of the E14 brain. In BaxΔTM-electroporated brains, in contrast, a relatively high proportion of GFP^+ cells

was detected in areas far from the ventricular zone, and astrocytic marker GFAP was seen for a subpopulation of the GFP^+ cells (Fig. 5d), indicating a preferential astrocytic specification of BaxΔTM-transfected precursors. Consistently, $GFAP^+$ cells among GFP^+ cells were significantly greater in the cortices transfected with BaxΔTM (Fig. 5f). This BaxΔTM-induced increase in astrocytes was accompanied by a significant reduction of $TuJ1^+$ neurons (Fig. 5e). This was in clear contrast to a significant decrease in $GFAP^+$ astrocytes observed for Bcl-X_LΔTM-transfected cortices. The quantification confirmed the above observation: percentages of $GFAP^+/GFP^+$ cells were 3.2% ± 0.4% (control), 2.2% ± 0.4% (Bcl-X_LΔTM), and 5.0% ± 0.8% (BaxΔTM), while percentages of $TuJ1^+/GFP^+$ cells were 94.1% ± 0.6% (control), 96.0% ± 0.5% (Bcl-X_LΔTM), and 91.1% ± 1.2% (BaxΔTM).

Intracellular signaling molecules activated in Bcl-X_L- and Bax-transduced cultures. Except for the caspase-mediated apoptosis pathway, intracellular signaling pathways downstream to Bcl-X_L/Bax have scarcely been characterized. The levels of activated (phosphorylated) forms of MAPK, Akt, signal transducer activators of transcription 1 and 3 (STAT1 and -3), and CREB in precursor cultures transduced with Bcl-X_L or Bax were examined. A striking change in the activation of these intracellular signal molecules was observed upon Bcl-X_L and Bax overexpression. Compared to what was seen for control cultures, increased levels of phosphorylated forms of MAPK, Akt, CREB, and STAT-1 were observed 2 days posttransduction for Bcl-X_L-transduced cultures. Bax overexpression also activated phosphorylation of Akt and STAT1 and -3 (Fig. 6a). In contrast to what was seen for the activation of CREB by Bcl-X_L, the level of phospho-CREB in Bax-transduced cultures was lower than that in the control cultures. Importantly, the activation patterns of these signal molecules in the cultures transduced with Bcl-X_LΔTM and BaxΔTM were similar to those for WT Bcl-X_L and Bax, respectively (Fig. 6b; also see Fig. S4 in the supplemental material). STAT1 and Akt activation was evident during precursor expansion in cultures transduced with Bcl-X_L and Bax but subsided during precursor differentiation (data not shown). In contrast, MAPK was activated only during the further differentiation period in Bax-transduced cultures (data not shown). These findings indicate that Bcl-X_L/Bax regulates the activation of signal molecules in a time- or differentiation stage-dependent manner.

Bcl-X_L/Bax alter the expression of bHLH transcriptional factors. Overexpression of Bcl-X_L in cultured E14 cortical precursors upregulated the expression of pro-neuronal basic helix-loop-helix (bHLH) transcription factors (Fig. 6c and d). In real-time PCR analyses, levels of Mash1, neurogenin 1 (Ngn1), and NeuroD proteins in Bcl-X_L-transduced cultures were enhanced 2.68 (± 0.08)-fold, 2.73 (± 0.31)-fold, and 2.24 (± 0.74)-fold, respectively, compared to control cultures (for each value, $n = 4$, $P < 0.001$, ANOVA). Conversely, Hes-1 and -5 and Id-1, -2, and -3, which antagonize neurogenesis, were significantly downregulated in Bcl-X_L-overexpressed precursor cells. The expression patterns of these bHLH transcriptional factors regulated by Bax were the opposite of those regulated by Bcl-X_L. Bax overexpression in the precursors led to the upregulation of anti-neuronal bHLH (1.59 [± 0.41]-fold in Hes1, 2.65 [± 0.48]-fold in Hes5, 1.91 [± 0.38]-fold in Id1, 1.38 [± 0.41]-fold in Id2, and 1.54 [± 0.39]-fold in Id3; for each value, $n = 4$, $P < 0.001$, ANOVA), while pro-neuronal bHLHs were downregulated (Fig. 6c and d). Messages for the genes involved in Notch signaling did not significantly differ among the groups. These findings indicate that Bcl-X_L/Bax proteins elicit their neurogenic/astrogenic actions by regulating activities of the bHLH transcription factors.

DISCUSSION

In the present study, we attempted to elucidate the role of Bcl-X_L/Bax proteins in the fate specification of embryonic cortical precursor cells. The increased neuronal yield by Bcl-X_L overexpression has previously been demonstrated for the cultures of mouse embryonic stem cells (27) and neural precursors isolated from a human embryo (17). The present study not only further consolidated the Bcl-X_L-mediated neuronal differentiation using gain- and loss-of-function studies but also uncovered the role of Bax in astrocyte formation during brain development. Our results strongly suggest that the neuronal versus glial fate determination of neural precursor cells is influenced if not determined by the balance of Bcl-X_L and Bax activities. Since the anti- and proapoptotic roles of Bcl-X_L and Bax proteins have been firmly established, an enhanced mechanism for selective survival and death for neuronally committed progenitors and/or neurons by Bcl-X_L and Bax, respectively, has been considered as a likely mechanism underlying the Bcl-X_L- and Bax-mediated precursor cell differentiation. However, our findings in this study provide strong evidence that rules out the possibility of the selective mechanism and instead suggests instructive roles of Bcl-X_L and Bax proteins in the fate specification of neural precursors. Evidence supporting instructive roles of the Bcl-2 family proteins could be summarized as follows. First, decreased numbers of astrocytes, as detected by specific markers, were observed for the developing cortices of Bax-KO mice (Fig. 1). Importantly, the absolute number of GFAP-positive astrocytes from Bax-KO embryonic cortices was smaller than that from WT cortices both in the flow cytometry analysis (Fig. 1c) and from cultures for differentiated precursor cells in vitro (Fig. 2). If the decrease in the number of astrocytes was due to increased astrocytic cell death, but not due to reduced formation of astrocytes, Bax can be assigned an antiapoptotic role of preventing the cell death of astrocytes. However, because Bax is a proapoptotic protein which plays a negative role in cell survival, the decrease of astrocytic cell numbers in Bax-KO mice is unlikely to be due to an apoptosis-mediated control of cell numbers. Therefore, these results, together with the astrocyte-to-neuron transition in the differentiation of Bax-KO precursors (Fig. 2a and b), strongly suggest an active role of Bax in astrocyte formation. Second, the findings obtained from the gain- and loss-of-function studies in vitro (Fig. 3), especially lineage analyses of clones derived from single cells, firmly support the role of Bcl-X_L in neuronal differentiation of the cortical precursors at the expense of astrocytic differentiation (Fig. 3c). Similar experiments with Bax likewise indicated that astrocytic differentiation at the expense of neuronal differentiation was promoted by Bax in cortical precursor cells (Fig. 3a and c; also see Fig. S3 in the supplemental material). Third, enhanced cell survival by the caspase inhibitors did not significantly alter the

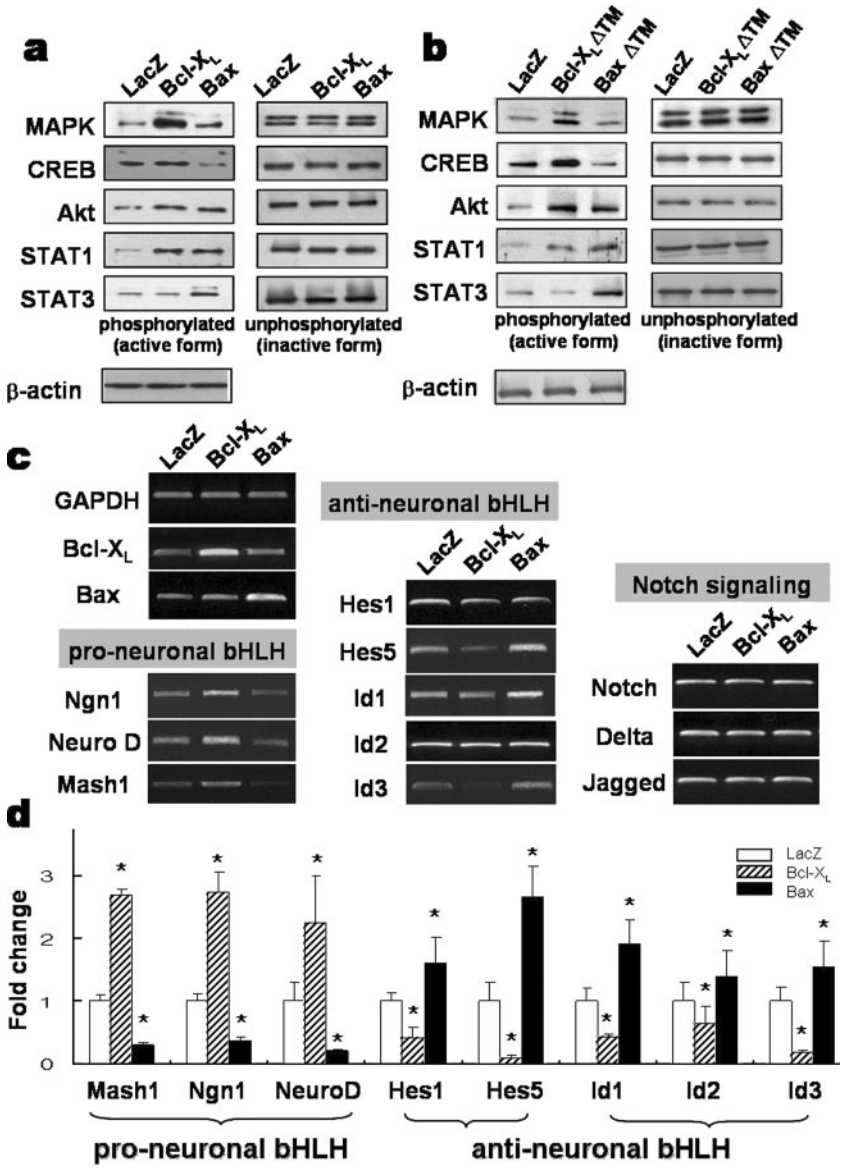

FIG. 6. Intracellular signal molecules and bHLH transcription factors altered during Bcl-X_L/Bax-mediated precursor differentiation. (a and b) Intracellular signal molecules activated by WTs (a) or truncated mutants (b) of Bcl-X_L/Bax. Each transduced culture was harvested 2 days after infection, and the immunoblot analyses were performed in the presence of the pan-caspase inhibitor z-VAD-FMK. Proteins were extracted on the last day of cell proliferation and differentiation and subjected to Western blot analysis. The immunoblots shown are typical examples from four or five independent experiments. (c and d) Bcl-X_L/Bax-induced expression patterns of the pro-/anti-neuronal bHLH transcription factors. In the presence of z-VAD-FMK, transduced precursors were proliferated for 2 days, and total RNA was extracted from each culture. Semiquantitative (c) and real-time (d) PCR analyses were performed to evaluate the expression of bHLH genes with proneural and antineural activities and Notch signaling pathway genes involved in neuron or astrocyte differentiation. As shown in panel c, the mRNA levels of candidate genes were analyzed by semiquantitative PCR, followed by gel electrophoresis and ethidium bromide staining. Results from SYBR real-time PCR analysis of identical genes are shown in panel d. Each gene expression value was normalized to GAPDH. Boxes and error bars represent mean and standard error values from six independent experiments. *, significantly different from LacZ transduced control at a P value of <0.001; ANOVA.

alternative lineage commitment induced by Bcl-X_L or Bax. Finally, the Bcl-X_L/Bax mutations at the sites critical for dimerization and mitochondrial localization of these Bcl-2 family proteins, which abolished their roles in the control of cell apoptosis, did not affect the precursor differentiation (Fig. 4). These findings together suggest that Bcl-X_L- and Bax-induced fate determination of neural precursor cells is separable from the roles of Bcl-X_L and Bax in the regulation of cell apoptosis and that Bcl-X_L and Bax play an instructive role in the fate determination of neural precursor cells.

Activation of intracellular extracellular signal-regulated kinase, phosphatidylinositol 3-kinase, CREB, and JAK/STAT pathways has been suggested to be responsible for neuronal and/or astrocytic differentiation (3, 10, 18, 19). In fact, we noticed significant Bcl-X_L- and Bax-mediated changes in the levels of the activated (phosphorylated) forms of these intra-

cellular molecules (Fig. 6a and b). While Akt and STAT1 were similarly activated in Bcl-X_L- and Bax-transduced cells, clear differential changes in the activation of several molecules were noticed. Specifically, MAPK and CREB were preferentially activated in Bcl-X_L-transduced cells, while STAT3 was selectively activated in Bax-transduced cultures (Fig. 6a and b; also see Fig. S4 in the supplemental material). Furthermore, the activated levels of these signal molecules were varied during the period of precursor differentiation in vitro (see Fig. S4 in the supplemental material). Therefore, the mechanisms underlying the Bcl-X_L- and Bax-induced precursor differentiation likely involve a complex web of several specifically and dynamically regulated signaling pathways. Examining the expression patterns of bHLH transcriptional factors known to be involved in neuronal and glial differentiation also provided further support for the new role of Bax and Bcl-X_L proteins (Fig. 6c and d). Proneural genes were upregulated by Bcl-X_L, and gliogenic genes were upregulated by Bax, suggesting that Bcl-X_L-mediated neuron and Bax-mediated astrocytic differentiations ultimately channel into the control of the bHLH factor expressions.

In conclusion, our data provide the initial evidence for an instructive role of the Bcl-2 family proteins played in the fate specification of neural precursor cells. Although detailed mechanisms for the differentiation effects largely remain to be uncovered, the results from this study connect the Bcl-2 genes to established intracellular signal molecules and transcriptional factors involved in neural development. The ways in which these signaling events interact and are ultimately relayed to gene expression for neuronal and astrocytic differentiation represent potentially interesting issues.

ACKNOWLEDGMENT

This work was supported by SC2150 (Stem Cell Research Center of the 21st Century Frontier Research Program) funded by the Ministry of Science and Technology, Republic of Korea.

REFERENCES

1. **Abe-Dohmae, S., N. Harada, K. Yamada, and R. Tanaka.** 1993. Bcl-2 gene is highly expressed during neurogenesis in the central nervous system. Biochem. Biophys. Res. Commun. **191:**915–921.
2. **Bittman, K. S., and J. J. LoTurco.** 1999. Differential regulation of connexin 26 and 43 in murine neocortical precursors. Cereb. Cortex **9:**188–195.
3. **Bonni, A., Y. Sun, M. Nadal-Vicens, A. Bhatt, D. A. Frank, I. Rozovsky, N. Stahl, G. D. Yancopoulos, and M. E. Greenberg.** 1997. Regulation of gliogenesis in the central nervous system by the JAK-STAT signaling pathway. Science **278:**477–483.
4. **Chang, M. Y., H. Son, Y. S. Lee, and S. H. Lee.** 2003. Neurons and astrocytes secrete factors that cause stem cells to differentiate into neurons and astrocytes, respectively. Mol. Cell. Neurosci. **23:**414–426.
5. **Chang, M. Y., C. H. Park, S. Y. Lee, and S. H. Lee.** 2004. Properties of cortical precursor cells cultured long term are similar to those of precursors at later developmental stages. Brain Res. Dev. Brain Res. **153:**89–96.
6. **Chang, M. Y., C. H. Park, H. Son, Y. S. Lee, and S. H. Lee.** 2004. Developmental stage-dependent self-regulation of embryonic cortical precursor cell survival and differentiation by leukemia inhibitory factor (LIF). Cell Death Differ. **11:**985–996.
7. **Chen, D. F., G. E. Schneider, J. C. Martinou, and S. Tonegawa.** 1997. Bcl-2 promotes regeneration of severed axons in mammalian CNS. Nature **385:**434–438.
8. **D'Mello, S. R., F. Aglieco, M. R. Roberts, K. Borodezt, and J. W. Haycock.** 1998. A DEVD-inhibited caspase other than CPP32 is involved in the commitment of cerebellar granule neurons to apoptosis induced by K+ deprivation. J. Neurochem. **70:**1809–1818.
9. **Gross, A., J. M. McDonnell, and S. J. Korsmeyer.** 1999. BCL-2 family members and the mitochondria in apoptosis. Genes Dev. **13:**1899–1911.
10. **Hermanson, O., K. Jepsen, and M. G. Rosenfeld.** 2002. N-CoR controls differentiation of neural stem cells into astrocytes. Nature **419:**934–939.
11. **Holm, K., and O. Isacson.** 1999. Factors intrinsic to the neuron can induce and maintain its ability to promote axonal outgrowth: a role for BCL2? Trends Neurosci. **22:**269–273.
12. **Jonas, E. A., D. Hoit, J. A. Hickman, T. A. Brandt, B. M. Polster, Y. Fannjiang, E. McCarthy, M. K. Montanez, J. M. Hardwick, and L. K. Kaczmarek.** 2003. Modulation of synaptic transmission by the BCL-2 family protein Bcl-X_L. J. Neurosci. **23:**8423–8431.
13. **Knudson, C. M., K. S. Tung, W. G. Tourtellotte, G. A. Brown, and S. J. Korsmeyer.** 1995. Bax-deficient mice with lymphoid hyperplasia and male germ cell death. Science **270:**96–99.
14. **Krajewska, M., J. K. Mai, J. M. Zapata, K. W. Ashwell, S. L. Schendel, J. C. Reed, and S. Krajewski.** 2002. Dynamics of expression of apoptosis-regulatory proteins Bid, Bcl-2, Bcl-X, Bax and Bak during development of murine nervous system. Cell Death Differ. **9:**145–157.
15. **Kretz, A., S. Kugler, C. Happold, M. Bahr, and S. Isenmann.** 2004. Excess Bcl-X_L increases the intrinsic growth potential of adult CNS neurons in vitro. Mol. Cell. Neurosci. **26:**63–74.
16. **Lindsten, T., J. A. Golden, W. X. Zong, J. Minarcik, M. H. Harris, and C. B. Thompson.** 2003. The proapoptotic activities of Bax and Bak limit the size of the neural stem cell pool. J. Neurosci. **23:**11112–11119.
17. **Liste, I., E. Garcia-Garcia, and A. Martinez-Serrano.** 2004. The generation of dopaminergic neurons by human neural stem cells is enhanced by Bcl-X_L, both in vitro and in vivo. J. Neurosci. **24:**10786–10795.
18. **Lonze, B. E., and D. D. Ginty.** 2002. Function and regulation of CREB family transcription factors in the nervous system. Neuron **35:**605–623.
19. **Menard, C., P. Hein, A. Paquin, A. Savelson, X. M. Yang, D. Lederfein, F. Barnabe-Heider, A. A. Mir, E. Sterneck, A. C. Peterson, P. F. Johnson, C. Vinson, and F. D. Miller.** 2002. An essential role for a MEK-C/EBP pathway during growth factor-regulated cortical neurogenesis. Neuron **36:**597–610.
20. **Minn, A. J., C. S. Kettlun, H. Liang, A. Kelekar, M. G. Vander Heiden, B. S. Chang, S. W. Fesik, M. Fill, and C. B. Thompson.** 1999. Bcl-X_L regulates apoptosis by heterodimerization-dependent and -independent mechanisms. EMBO J. **18:**632–643.
21. **Motoyama, N., F. Wang, K. A. Roth, H. Sawa, K. I. Nakayama, K. Nakayama, I. Negishi, S. Senju, Q. Zhang, and S. Fujii.** 1995. Massive cell death of immature hematopoietic cells and neurons in Bcl-x-deficient mice. Science **267:**1506–1510.
22. **Parnavelas, J. G.** 1999. Glial cell lineages in the rat cerebral cortex. Exp. Neurol. **156:**418–429.
23. **Sauvageot, C. M., and C. D. Stiles.** 2002. Molecular mechanisms controlling cortical gliogenesis. Curr. Opin. Neurobiol. **12:**244–249.
24. **Sawada, M., P. Hayes, and S. Matsuyama.** 2003. Cytoprotective membrane-permeable peptides designed from the Bax-binding domain of Ku70. Nat. Cell Biol. **5:**352–357.
25. **Seidenfaden, R., A. Desoeuvre, A. Bosio, I. Virard, and H. Cremer.** 2006. Poor survival of adult SVZ cell than neonatal SVZ cells. Glial conversion of SVZ-derived committed neuronal precursors after ectopic grafting into the adult brain. Mol. Cell. Neurosci. **32:**187–198.
26. **Sergent-Tanguy, S., C. Chagneau, I. Neveu, and P. Naveilhan.** 2003. Fluorescent activated cell sorting (FACS): a rapid and reliable method to estimate the number of neurons in a mixed population. J. Neurosci. Methods **129:**73–79.
27. **Shim, J. W., H. C. Koh, M. Y. Chang, E. Roh, C. Y. Choi, Y. J. Oh, H. Son, Y. S. Lee, L. Studer, and S. H. Lee.** 2004. Enhanced in vitro midbrain dopamine neuron differentiation, dopaminergic function, neurite outgrowth and MPP+ resistance in mouse ES cells overexpressing Bcl-X_L. J. Neurosci. **24:**843–852.
28. **Shimazaki, T., T. Shingo, and S. Weiss.** 2001. The ciliary neurotrophic factor/leukemia inhibitory factor/gp130 receptor complex operate in the maintenance of mammalian forebrain neural stem cells. J. Neurosci. **21:**7642–7653.
29. **Shimizu, S., T. Kanaseki, N. Mizushima, T. Mizuta, S. Arakawa-Kobayashi, C. B. Thompson, and Y. Tsujimoto.** 2004. Role of Bcl-2 family proteins in a non-apoptotic programmed cell death dependent on autophagy genes. Nat. Cell Biol. **6:**1221–1228.
30. **Srinivasan, A., L. M. Foster, M. P. Testa, T. Ord, R. W. Keane, D. E. Bredesen, and C. Kayalar.** 1996. Bcl-2 expression in neural cells blocks activation of ICE/CED-3 family proteases during apoptosis. J. Neurosci. **16:**5654–5660.
31. **Sun, W., T. W. Gould, S. Vinsant, D. Prevette, and R. W. Oppenheim.** 2003. Neuromuscular development after the prevention of naturally occurring neuronal death by Bax deletion. J. Neurosci. **23:**7298–7310.
32. **Sun, W., A. Winseck, S. Vinsant, O. H. Park, H. Kim, and R. W. Oppenheim.** 2004. Programmed cell death of adult-generated hippocampal neurons is mediated by the proapoptotic gene Bax. J. Neurosci. **24:**11205–11213.
33. **Tropepe, V., M. Sibilia, B. G. Ciruna, J. Rossant, E. F. Wagner, and D. Van der Kooy.** 1999. Distinct neural stem cells proliferate in response to EGF and FGF in the developing mouse telencephalon. Dev. Biol. **208:**166–188.
34. **Tsai, R. Y., and S. Kim.** 2005. Fibroblast growth factor 2 negatively regulates the induction of neuronal progenitors from neural stem cells. J. Neurosci. Res. **82:**149–159.
35. **Vekrellis, K., M. J. McCarthy, A. Watson, J. Whitfield, L. L. Rubin, and J.**

Ham. 1997. Bax promotes neuronal cell death and is downregulated during the development of the nervous system. Development **124:**1239–1249.
36. **Wang, K., A. Gross, G. Waksman, and S. J. Korsmeyer.** 1998. Mutagenesis of the BH3 domain of BAX identifies residues critical for dimerization and killing. Mol. Cell. Biol. **18:**6083–6089.
37. **Weiss, S., C. Dunne, J. Hewson, C. Wohl, M. Wheatley, A. C. Peterson, and B. A. Reynolds.** 1996. Multipotent CNS stem cells are present in the adult mammalian spinal cord and ventricular neuroaxis. J. Neurosci. **16:**7599–7609.
38. **Wolter, K. G., Y. T. Hsu, C. L. Smith, A. Nechushtan, X. G. Xi, and R. J. Youle.** 1997. Movement of Bax from the cytosol to mitochondria during apoptosis. J. Cell Biol. **139:**1281–1292.
39. **Yuan, J., and B. A. Yankner.** 2000. Apoptosis in the nervous system. Nature **407:**802–809.
40. **Zaidi, A. U., C. D'Sa-Eipper, J. Brenner, K. Kuida, T. S. Zheng, R. A. Flavell, P. Rakic, and K. A. Roth.** 2001. Bcl-X(L)-caspase-9 interactions in the developing nervous system: evidence for multiple death pathways. J. Neurosci. **21:**169–175.
41. **Zerlin, M., S. W. Levison, and J. E. Goldman.** 1995. Early patterns of migration, morphogenesis, and intermediate filament expression of subventricular zone cells in the postnatal rat forebrain. J. Neurosci. **15:**7238–7249.
42. **Zufferey, R., D. Nagy, R. J. Mandel, L. Naldini, and D. Trono.** 1997. Multiply attenuated lentiviral vector achieves efficient gene delivery in vivo. Nat. Biotechnol. **15:**871–875.